Penerbit Akademia Baru

Journal of Advanced Research in Fluid Mechanics and Thermal Sciences

Journal homepage: www.akademiabaru.com/arfmts.html
ISSN: 2289-7879

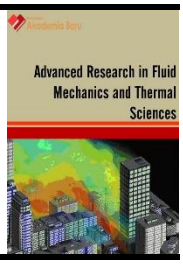

Effect of Hemodynamic Parameters on Physiological Blood Flow through Cardiovascular Disease (CVD) – The Perspective Review

Open Access

Nur Afikah Khairi @ Rosli[1], Mohd Azrul Hisham Mohd Adib[1,*], Nur Hazreen Mohd Hasni[2], Mohd Shafie Abdullah[3]

[1] Medical Engineering & Health Intervention Team (MedEHiT), Department of Mechanical Engineering, College of Engineering, Universiti Malaysia Pahang, 26600 Pekan, Pahang, Malaysia
[2] Family Health Unit, Pahang Health State Department, Malaysia Ministry of Health, Jalan IM 4, Bandar Indera Mahkota, 25582 Kuantan, Pahang, Malaysia
[3] Department of Radiology, School of Medical Sciences, Health Campus, Universiti Sains Malaysia, 16150 Kubang Kerian, Kelantan, Malaysia

ARTICLE INFO

Article history:
Received 20 December 2019
Received in revised form 26 April 2020
Accepted 27 April 2020
Available online 15 August 2020

Keywords:
Coronary artery disease; hemodynamics; physiological blood flow; computational study

ABSTRACT

One of the cardiovascular diseases (CVD) that affect the heart is coronary artery disease (CAD). CAD is the disease that leads to fetal death due to plaque formation which blocked blood that carries oxygen to the human body. The tremendous trends of death in cardiovascular disease become worrisome to cardiologists and medical practitioners. Thus, many researchers grab the initiative to study the cardiovascular hemodynamic parameters such as wall shear stress (WSS), blood velocity, endothelial shear stress (ESS), and strain rate in identifying coronary artery disease factors. This paper aims to investigate the hemodynamic parameters that lead to the formation of coronary artery disease and the effect of the parameters on the physiological blood flow. Few research papers were investigated and analyzed by comparing numerical data and images from CFD analysis. Based on the study, the main hemodynamic parameter that produced the formation of coronary artery disease are wall shear stress and related proportionally with velocity, shear stress, and strain rate factors. The result shows the low wall shear stress (WSS) developed the high formation of plaque in the coronary artery and will develop stenosis in an artery leading to a decrease of lumen size and increase of velocity near the plaque region. In conclusion, the evolutions of computational hemodynamic study are bringing huge contributions in identifying coronary artery disease and show a significant relationship with physiological blood flow.

* *Corresponding author.*
E-mail address: azrul@ump.edu.my

https://doi.org/10.37934/arfmts.74.1.1934

1. Introduction

Nowadays, coronary artery disease (CAD) is the leading cause of morbidity and mortality in developing countries [1]. The World Health Organization (WHO) had reported cardiovascular diseases (CVDs) are the number one cause of death worldwide, with an estimated 17.9 million deaths per year that include heart disease, stroke, rheumatic heart disease, and other conditions [2]. In Malaysia, the Star online had published an article regarding the heart attack that remains the leading cause of deaths with a total of 18,267 deaths or 15.6 % reported by the Department of Statistics Malaysia (DOSM) [3]. CAD refers to a disease that occurs due to the formation of lesions of plaque inside of the vascular wall, placed in the human heart. Factors that induce the formation of CAD mainly cause by unhealthy lifestyles and other systemic factors (e.g., raised blood glucose, blood pressure, obesity, smoking) [4]. As heart providing access to oxygen, nutrients and act as blood transporter to the human whole body, the heart vessel become one of the vital components in the heart itself. However, with the presence of the plaque in the vessel, the heart cannot fully function causing abruption of heart or known as myocardial infarction (MI) in the worst cases. The severity of plaque depends on the percentage of stenosis that occurs in a patient's coronary artery. Some research [5-7] studies about the composition of plaques, but using different methods. Numerical and computer simulation has been used in research [5] to determine the effect of stenosis of flow rates. The percentage of stenosis use for the research are 0%, 20%,35%,50%,70% and 90 %. Intravascular ultrasound (VH-IVUS) is used in *Habib Samady et al.,* [6] research by making a comparison of wall shear stress (WSS), plaque area, necrotic area, dense calcium area, fibrous area and fibrofatty area for 6 months with twenty patients of CAD. *Adib M.A.H.M et al.,* [7] have been experimenting to visualize the blockage of a coronary artery using *CardioVASS* device with plaque composition of 20%, 40%, 60%, and 90%. The study shows that the high deposition rate of plaque will disturb the flow of blood to the ends of coronary arteries. To understand the effect of the plaque distribution whether in physiological blood flow or hemodynamically, we refer to the computational fluid dynamics (CFD) methods that have been used widely for the research of CVDs. CFD is a feasible method that has been used for ages [1,5,8-12] in determining fluid flow and 3D model of coronary arteries. Besides studying about factors stimulating CAD such as bifurcations of coronary artery angles [5,9,11,12], image segmentation [8] and using finite element simulations [10], CFD can simulate an accurate flow of coronary arteries based on any parameter given. Physiological blood flow effected when deposition of plaque happens and causing smooth profile muscle proliferation simultaneously reduces the luminal diameter of endothelial dysfunction. Hemodynamics in cardiovascular supplies and driving the force for all blood flow in the body. The cardiovascular hemodynamics also represents the governing principle of blood flow (eg. Navier-Stokes equation, Murray's law, conservation of mass, conservation of energy, etc) and behavior in the blood vessel (Newtonian and Non-Newtonian). Navier-Stokes equation describes the viscous motion of fluids [13] while Murray's law describes restrictions of size relation and flow distributions in vessel network bifurcations [14]. Physiologically, this means that the blood flow in the cardiovascular system is equal to the change of blood pressure divided by the system resistance. Several researchers [15,16] have done comparative studies of cardiovascular hemodynamics for linear and nonlinear models. They observed, the heart valve shows drastic differences in blood flow patterns and hence differences of stresses causing impact at leaflets and vascular wall [17].

In this paper, we are studied and reviewed the importance of hemodynamic parameters that initiates the formation of CAD simultaneously to investigate the effect of the parameters on the physiological blood flow.

2. Methodology

2.1 Data Extraction and Analysis

This paper focused on the agreements of authors regarding variable hemodynamic parameters that initiates the formation of CAD. Most of the previous researchers are used multiple methods in determining hemodynamic parameters for CAD studies. Some of the authors are using VH-IVUS, X-ray angiographic method and computed tomography (CT) scan before transferred the actual imaging of vessels into digital imaging and communication in medicine (DICOM) and CFD. Other methods used are by choosing a particular number of patients of CAD undergoing a selective period for observations. Here, the author may observe any unusual changes in the CAD in a long-term period.

CFD is a tool that has been used for decades in simulation and fluid flow processes. Many researchers consider this method while underwent experimental and simulation investigation for their research as it is time-consuming and low in cost [8,11,12,18-20]. This CFD method not only limited to the selective field such as the mechanical and fluid field but also brings a great contribution to medical fields. Using the CFD method, the user can extract images from scanner such as CT scan, angiographic scan, VH-IVUS and others for real-simulation experiences. A complex calculation that reached thousands or millions of values can easily be done using the CFD software. However, the limitations that the user may experience are difficulties in setting the parameters of CFD such as setting-up for meshes, velocities of fluid and others. The small changes in setting may affect the numerical results at the end of the simulation.

2.2 Materials and Specifications

A computational study of blood flow analysis was conducted by Radhe Tado *et al.,* [11] using CT scan data assisted by MIMICS Research 19.0 and CFD analysis ANSYS FLUENT-14.5. The actual coronary arteries were extracted and created a new geometry of coronary arteries. The mathematical modeling principals used were Navier-Stokes equations and the continuity equation for an incompressible fluid. Based on his research, the areas of high WSS and high flow velocities were parallel to the plaques deposition. An analysis was conducted by Thanapong Chaichana *et al.,* [12] to investigate the hemodynamic effect of simulated plaques in left coronary artery models. A patient suspected with CAD problems was chosen before underwent a multislice angiography scan. ANSYS CFX-CFD package (version 12-ANSYS.Inc.) was used to solve Navier-Stokes equations. The results show that the flow velocity increased significantly due to the resultant lumen stenosis with WSS contour values ranged from 0 Pa to 3.50 Pa observed in both Newtonian and non-Newtonian fluid models. Mohammad Nouri *et al.,* [8] in his research suggested that low-density lipoproteins (LDL) in the vessel walls as the initiator of atherosclerosis and CAD problems. Simulated Non-Newtonian blood flow through normal and hypertensive conditions was reconstructed from CT images. Plasma flow and LDL transport were presented using Darcy's law and convection-diffusion-reaction equation, respectively. The results show that the LDL molecules sub-endothelial concentration was increased at local WSS, and maximized at the branch location. Results obtained by Guiying *Liu et al.,* [18] found that low WSS and wall pressure gradient (WPG) at bifurcations regions coincide with the plaques points, therefore confirming the correlation between arterial geometry variation and fluid mechanical properties. From the research analysis, it was found that low WSS regions' values are less than or equal to 0.4 Pa while high WSS values were more than or equal to 40 Pa, which occurs at the inner wall and bifurcation angles respectively. Arnav Kumar *et al.,* [19] studying the relationship between severe endothelial dysfunction (EDFx) found that low WSS was greatly contributed with severe EDFx with 71% compared to intermediate WSS (22%) and high WSS

(23%). All 44 patients from the research conducted coronary angiography, fractional flow reserve (FFR) and endothelial function testing. Wellnhofer *et al.,* [21] were investigating characterize patterns of local WSS with different types of remodeling in coronary arteries succeed in grouping the WSS values by identifying the percentage of the exposed luminal region with WSS≤0.4 Pa, WSS≥1.5 Pa and WSS≥15 Pa representing the low, medium and high WSS respectively. The flow simulation was conducted with five patients with CAD, five patients with aneurysmatic CAD (AnCAD) and right coronary arteries developed from seven controls (seven patients).

3. Results

3.1 Principle Outcome: Comparison of Methods, Equations, and Findings

The summarization of methods, equations, and findings visible in Table 1 and Table 2. All of the authors focused on the contribution of low WSS and additional aims and relationships (EDFx, biomechanical forces, etc.,) that related to their research respectively. Based on the tables, we can observe that the common equations used in solving problems related to the low WSS and fluids are Navier-Stokes equation and continuity equation that represents the blood flow. Newtonian and non-Newtonian blood models are also compared in Thanapong Chaicana *et al.,* [12] paper, where there are almost similar values for WSS in both blood models, representing huge similarities in WSS values although having different blood models. Based on the [11,12,8,18,19,21] papers, we can find a mutual agreement of the authors regarding hemodynamic parameters related significantly to the physiological blood flow. Details of the studies can be observed in Table 1 and Table 2.

Table 1
Details of studied articles

Article, Year	Patients Age (years old)	Method	Results	Findings
Radhe Tado *et al.,* [11], 2018	The geometry of suspected CAD patients was extracted from the CT scan for remodeling	A CT scan was used to construct a new geometrical model of left coronary arteries (LCA). MIMICS Research 19.0 and CFD analysis of ANSYS FLUENT-14.5 were used	The authors used a velocity of inlet values was 0.25 m/s and the maximum velocity was 0.30 m/s. Results presented a higher velocity at a post-plaque area, with a decrease in luminal inlet regions. The WSS showed decreased values in distal segments and pressure drops significantly in stenotic segments	Plaques mostly occurred at bifurcations areas, side branches and preferred outer wall of vessel walls. Thus, the increase of WSS and greater velocities near the plaques developments regions
Thanapong Chaichana *et al.,* [12], 2012	Data were taken from a sample of suspected CAD patients who went under multislice CT angiography scan	Extraction of the left coronary model of patient's data using CT scan, DICOM software, Analyze 7.0 software and ANSYS ICEM CFD version 12 software. The authors also applied MATLAB and CFD CFX Command Language programming to define boundary	High flow velocities were found due to the resultant lumen stenosis occurred. PSG values recorded ranged from 459.29-800 kg/m^2 to 345.71 – 629.64 kg/m^2 significantly with the presence of the plaque. PSG values became low with readings range	The results presented various ranges of values for WSS, PSG and velocities values. The authors also compared values of Newtonian and non-Newtonian blood model that showing almost a huge gap of all the parameters values mentioned earlier with

		condition and velocities of fluids	from 61.79-118.57 kg/m^2s^2 to 5-61.79 kg/m^2s^2. Velocity values increased from 23.96 to 30.50 mm/s at plaques region during systolic peak. The mid-diastolic phase showed incremental values from 28.32 to 30.50 mm/s. WSS values range from 0.50 -1.75 Pa with a non-Newtonian blood model and from 0.50 Pa -0.75 Pa with a Newtonian blood model.	the presence of plaques on the geometrical models. Consequently, the blood circulation became obstructed and disrupted the velocity values as main parameters in determining WSS values
Mohammad Nouri *et al.,* [8], 2015	49 years old male patients (Kosar hospital in Shiraz) using 64-slice Philips CT machine	A design of schematic computational domains was simulated to observe filtration flows of LDL and blood plasma. The mechanism of the model included the endothelium layer with three- pores model.	Data recorded that the percentage of the total flows was 5%, 7%, 14%, 23%, and 51% respectively. Results showed that there was disturbed blood flow in the measurements where irregularities of velocity and WSS values occurred. Average WSS and hypertensive WSS were 0.45 Pa and 0.92 Pa respectively. Focused on the biomechanical forces, low WSS contributed to the formation of mitosis of endothelial cells and formed leaky junctions incidence. Plasma flow released through leaky junctions and interrupted sub-endothelial aggregation of LDL molecules	Findings showed that the formation of low WSS interrupted other cells and components that vital to the human body, as well as biomechanical forces. The dependent relationship between WSS, velocities, and relation with biomechanical forces was showed in this paper
Guiying Liu *et al.,* [18], 2015	Remodeling based on an anatomical model of CAD patients	Based on a real anatomical model, the authors designed 125 new idealized models with variable angulations (60, 75, 90, 105, 120 degrees) and curvatures (30, 60, 90, 120 and 150 degrees). The mesh had been generated by a software "(ANSYS Inc., Canonsburg, PAUSA)". Cardiac CT imaging was used with 64-detector row helical scanner (Aquilion 64,	Result found that high WSS (WSS ≥ 40 Pa) mostly occur at the root of the side-branch next to the bifurcation regions, while low WSS (WSS≤0.4 Pa) mainly located at the outer and inner wall. The changes in angulation and curvatures affected the WSS values and increased risk of the development of	There was a significant relationship between the hemodynamics changes with different angulations and curvatures of vessel structures.

		Toshiba Medical Systems, Otawara, Japan)	vulnerable atherosclerosis	
Arnav Kumar *et al.,* [19], 2018	44 patients diagnosed with CAD underwent EDFx testing, coronary angiography, and FFR testing.	3D Geometrical reconstructions using QAngio XA 3D RE (Medis Medical Imaging Systems, Leiden, the Netherlands) Meshing process using the finite element library LifeV Acetylcholine (Ach) infusion was used to determine the severity of EDFx in patients. Patients with >10% vasoconstriction were identified as severe EDFx cases Low WSS were defined with (<1 Pa), intermediate (1 to 2.5 Pa), or high (>2.5 Pa)	The median age of patients was 52 years old. FFR mean values were 0.94±0.06, the WSS median was 3.67 Pa. 24% was the total EDFx severity of patients. Low WSS showed a higher percentage (71%) of severe EDFx rather than intermediate (22%) and high WSS (23%).	Low WSS had a high percentage in severe EDFx cases compared to intermediate and high WSS The severity of EDFx related to the low WSS until reached WSS values of < 1 Pa Low WSS was non-linear with the severity of EDFx
E.Wellnhofer *et al.,* [21], 2009	Controls are 7 patients (4 female, age 52±17 years) CAD group consist of 5 patients (one female, age 50±10 years) The aneurysmatic group comprises of 5 patients (one female, 58±14 years)	Retrospective data analysis CFD flow FLUENT 6 (ANSYS Fluent Inc.Lebanon, USA) analysis (biplane angiographic projections)	Data showed that aneurysmatic CAD largely exposed to low WSS, while CAD graph shows elevated WSS trends	WSS affect the reconstruction of blood vessels Severe cases demonstrated WSS < 0.4 Pa Patients with obstructive diseases showed WSS > 15 Pa exposed luminal area

Table 2
Equation involved in studied articles

Article, Year	Equation	Numerical Equation	Notes
Radhe Tado *et al.,* [11], 2018	Navier-Stokes equation Continuity equation for incompressible fluid Non-Newtonian blood model Carreau model	Navier-Stokes equation: $\rho\left(\frac{dv}{dt}+V.\nabla V\right)=-\nabla\tau-\nabla P)$ [22] Continuity equation: $\nabla.V=0$ [23] Non-Newtonian Carreau model $\mu(x,t)=\mu_\infty+(\mu_o-\mu_\infty)\left[1+(\lambda\dot{\gamma}(x,t)^a\right]^{\frac{n-1}{a}})$ [24] V is two-dimensional velocity vector,t the time, Prefer to the pressure, ρ is density, τ is the stress tensor, μ_o is the zero-shear rate viscosity, μ_∞ is the infinite shear rate viscosity, λ is a parameter and n refer to the dimensionless parameter	A Carreau model was used to compare two different Newtonian and non-Newtonian flows with a simpler and steady oscillatory flow in straight and curved pipe geometries [25]. The authors stated that Carreau models can predict hemodynamics parameters more accurately.
Thanapong Chaichana *et al.,* [12], 2012	Newtonian and non-Newtonian blood model Generalized power law The magnitude of local pressure gradient Navier-Stokes equation	Newtonian,non-Newtonian blood model equation and generalized power law equation: $\mu=\lambda(\dot{\gamma}\mid\dot{\gamma}\mid^{n(y)-1}$ $\lambda(\dot{\gamma})=\mu_\infty+\Delta\mu\exp\left[-\left(1+\frac{\mid\dot{\gamma}\mid}{a}\right)\exp\left(\frac{-b}{\mid\dot{\gamma}\mid}\right)\right]$, $n(\dot{\gamma})=n_\infty+\Delta n\,\mathrm{ex}\left[t-\left(1+\frac{\mid\dot{\gamma}\mid}{c}\right)\exp\left(\frac{-d}{\mid\dot{\gamma}\mid}\right)\right]$, [26] The magnitude of the local pressure gradient: $\sqrt{(\frac{dp}{du})^2+(\frac{dp}{dv})^2+(\frac{dp}{dw})^2}$ [27] p is defined as the pressure in the area of the interest, u,v,w, are referring to the Cartesian x,y,z coordinates in blood flow velocity	No notes available
Mohammad Nouri *et al.,* [8], 2015	Continuity equation Navier-Stokes equation Generalized power law The fraction of leaky cells Kedem-Katchalsky equation Hydraulic conductivity Diffusive permeability of leaky junctions	Continuity and Navier-Stokes equation: $\nabla.V_1=0$; [28] $\rho_b(V_1.\nabla V_1)=-\nabla.\tau-\nabla p_1$ [29] Generalized power law: $\mu_b=0.1\,\dot{\gamma}^{n-1}$ [30] $\lambda(\dot{\gamma})=0.035+0.25\exp\left[-\left(1+\frac{\mid\dot{\gamma}\mid}{50}\right)\exp\left(\frac{-3}{\mid\dot{\gamma}\mid}\right)\right]$, [31] $n(\dot{\gamma})=1.0-0.45\exp\left[-\left(1+\frac{\mid\dot{\gamma}\mid}{50}\right)\exp\left(\frac{-4}{\mid\dot{\gamma}\mid}\right)\right]$ [32] Fraction leaky cells equation: $\phi=\frac{area\ of\ leaky\ cells}{area\ of\ endothelial\ cells}=$ $(\#LC)\left(\frac{area\ of\ the\ area\ of\ one\ endothelial\ cell}{of\ all\ endothelial\ cells}\right)$ [23] Kedem-Katchalsky equation: $J_{v,i}=L_{p,i}\left(\Delta P^{end}-\sigma_{d,i}\Delta\pi^{end}\right)$ [33] $J_{s,i}=P_{diff,i}\Delta C^{end}+\left(1-\sigma_{f,i}\right)J_{v,j}\overline{C}^{end}$ [34] Hydraulic conductivity equation: $L_{p,lj}=\frac{4w^3}{3r_{cell}\mu_p l_{lj}}.\phi$ [35] Diffusive permeability of leaky junctions:	Variously referred equations from other authors were cited in this paper to achieve mutual understanding regarding the equation for arterial lumen and the three-pore model presented in this paper

	Diffusion coefficient equation	$P_{diff,1j} = \frac{area\ of\ leaky\ junctions}{are\ of\ all\ endothelial\ cells}(1-\alpha_{lj})P_{diff,slj}$ [26]	
	Darcy's law Convection-diffusion equation	Diffusion coefficient through leaky junction equation: $D_{lj} = D_l(1-\alpha_{lj})(1-1.004a_{lj}+0.418a_{lj}^3-0.169a_{lj}^5)$ [10] Darcy's law equation: $V_w = \frac{K_p}{\mu_P}\nabla P_w$ [36] $\nabla . V_w = 0$ [37] Convection-diffusion equation: $K_{lag}V_w\nabla C_w - D_w\nabla C_w + \tau_w C_w = 0$ [38] Generally, V_1 is the velocity vector, ρ_1 is the pressure, ρ_b is defined as blood density, τ is the stress tensor, μ_b is the blood viscosity, $J_{v,i}$ is the volume flux, $J_{s,i}$ is the solute flux, $L_{p,i}$ is the hydraulic conductivity, ΔP^{end}, $\Delta\pi^{end}$, ΔC^{end} are the pressure drop, osmotic pressure difference and the solute concentration difference across the endothelium layer, $\overline{C}^{end}$. $P_{diff,i}$ is the solute permeability through the pathway, $\sigma_{d,i}$ and $\sigma_{f,i}$ are the osmotic and solvent reflection coefficients, respectively. The w is the width, r_{cell} is the radius of leaky junctions, l_{lj} is the length of the leaky junctions, V_w is the velocity vector of transmural flow, P_w is the pressure within the wall, K_p is constant ($1.2\ x\ 10^{-18}m^2$), μ_p is constant (0.001 Pa s), C_w is the LDL concentration with the wall, K_{lag} is constant = 0.1486 is the LDL coefficient, $D_w = 8.0\ x\ 10^{-13}m^2s^{-1}$ is the effective diffusivity of LDL molecules trough arterial wall and $r_w = 3.0\ x\ 10^{-4}s^{-1}$ is the consumption rate constant of LDL molecules	
Guiying Liu *et al.,* [18], 2015	Newtonian fluid blood model Continuity and incompressible Navier-Stokes equation	Continuity and incompressible Navier-Stokes equation $\rho\frac{dv}{dt} + \rho(v.\nabla)v = -\nabla P + \rho g + \mu\nabla^2 v$ [28] $\nabla . v = 0$ [9] u refer to the fluid velocity vector, P is fluid pressure, ρ is blood density, v is velocity, ∇^2 is Laplacian operator, μ is dynamic viscosity, g is the gravity constant	The authors used the ratio of WSS and $\overline{WSS}$, the ratio parameter of pressure drop between the proximal inlet with peak systole of the distal outlet to the identified surface response curve
Arnav Kumar *et al.,* [19], 2018	Blood assumed to be incompressible Newtonian blood Incompressible Navier-Stokes equation Murray's law	Navier-Stokes equation: $\frac{du}{dt} + u.\nabla = -\frac{\nabla P}{\rho} + v\nabla^2 u$ [39] Murray's law $D_1^{3*} = D_2^{3*} = D_3^{3*}$ [40,41] u refer to the fluid velocity vector, P is fluid pressure, ρ is the fluid density, v is kinematic viscosity while ∇^2 is Laplacian operator D refers to the diameter of the arterial branch	Based on the paper context, Murray's law is defined as weights of the flux of the arterial branch, including the distal portion of the target vessel, concerning the neighbor [40,41]

E. Wellnhofer *et al.,* [21], 2009	Steady flow Navier-Stokes (momentum and mass conservation) Blood modeled with Newtonian Reynold's number	Navier-Stokes equation: $\frac{du}{dt} + u.\nabla = -\frac{\nabla P}{\rho} + v\nabla^2 u$ [34] Reynold's number $Re = \frac{\rho U l}{\mu}$ u refer to the fluid velocity vector, P is fluid pressure, ρ is the fluid density, v is kinematic viscosity while ∇^2 is Laplacian operator	No notes available

3.2 Secondary Outcome: Hemodynamic Parameters and Blood Flow Patterns

Hemodynamics can be defined as physical principles governing the movement of blood through the circulatory system [42-44]. The related hemodynamic parameters that contribute to the formation of CAD usually differ inflow of blood (laminar flow, turbulent flow, etc), shear stress and oscillatory flows [45]. Each of the parameters is highly crucial as small changes in the parameters will bring adverse effects on one's health. Vanderlaan *et al.,* [45] state that the areas of the laminar flow are parallel with the development of plaques. Although the hemodynamic parameters are not the only factors, the authors achieve an agreement where they are the pioneer in the development of the lesions [45]. Meanwhile, blood flow patterns described the behavior of the blood. Newtonian and non-Newtonian blood are examples of widely used principles in determining blood flow in experimental and simulation cases. These blood principles mainly include the viscosity level and shear rates of blood flow. Table 3 shows summarize the hemodynamic parameter definitions and the patterns of blood flow that are related to this research.

Table 3
The terminology of arterial hemodynamics [31]

Terms	Definition
Endothelial shear stress (ESS)	The tangential force derived by the friction of the flowing blood on the endothelial surface. It is the product of the shear rate at the wall and the blood viscosity (μ).
Shear rate	The spatial gradient of blood velocity, which describes how fast the blood velocity increases from areas at the arterial wall toward areas at the center of the lumen (ie, dv/dy, where dv is changed inflow velocity unit and dy is changed in the unit of radial distance from the wall). Physiologically, the shear rate decreases at the center of the lumen and gradually increases toward the wall.
Newtonian blood behavior	Constant blood viscosity independent of shear rate. In large-sized arteries (e.g., aorta) blood behaves largely in a Newtonian fashion.
Non-Newtonian blood behavior	Non-constant blood viscosity was inversely related to the shear rate. Blood has non-Newtonian properties, especially in veins, small-sized arteries, and in the microcirculation.
Laminar flow	Smooth, streamlined blood flow where viscous forces prevail against inertial forces.
Undisturbed laminar blood flow	Smooth streamlined flow characterized by concentric layers of blood moving in parallel along the course of the artery. The highest velocity is found at the center of the lumen, whereas the lowest velocity occurs along the wall. Uniform laminar blood flow primarily occurs in relatively straight arterial segments.
Disturbed laminar blood flow	Disturbed laminar flow characterized by reversed flow (I.e, flow separation, recirculation, and reattachment to forward flow). Disturbing laminar flow occurs in arterial segments with geometric irregularities (e.g., curvatures, branches, bifurcations), or upstream and downstream of stenosis.
Turbulent blood flow	Flow in which the blood velocity at any given point varies continuously over time, even though the overall flow is steady. In turbulent flow, the inertial forces are more significant than viscous forces. Turbulent blood flow rarely occurs but has been described in the human aorta at peak

	systole, during heavy exercise in much of the central arterial system, distal to severe stenosis (>75 %), and in aneurysms.
Steady blood flow	Blood flow in which velocity does not vary with time. This type of flow does not occur in vivo; however, it has been largely used in computational fluid dynamic studies.

4. Discussion

4.1 Hemodynamic Parameters

Hemodynamic parameters such as WSS mainly become the relevant parameter that initiates problems related to the CVDs. VanderLaan *et al.,* [45] in their paper stated the hemodynamic parameters encourage the formation of atherosclerosis accompanied by other factors for instance changes in the arterial vasculature. Consequently, resulting in unparalleled flow parameters in vasculature regions. The assumptions were supported by Wellnhofer *et al.,* [21] where they claimed the WSS had a significant effect on the remodeling of the vessel wall. The results from their research showed in severe cases, WSS values reached less than 0.4Pa and become worst with obstructive patients, WSS values increased tremendously with values higher than 15 Pa. These conditions proved the importance of WSS and geometrical modeling respectively. The research made by *Arnav Kumar et al.,* [19] who studies the relationship between EDFx and WSS identified the low WSS had a higher percentage in severe EDFx cases rather than intermediate and high WSS. Jacques Ohayon *et al.,* [46] explained the local arterial wall was related to the WSS and flow-induced shear stress by the pressure of the blood and contraction of myocardial. The research studied by Guiying *Liu et al.,* [18] focused on bifurcation and angulations areas with WSS. From their research, they had concluded the low WSS commonly occurred at the inner and outer wall of coronary vessels with WSS less than 0.4Pa and high WSS mostly occurred at bifurcation regions with WSS more than 40Pa. The statements regarding developments of WSS at bifurcations areas were proven by Radhe Tado *et al.,* [11] who confirmed the plaques distribution mostly happened at complex curvatures and near bifurcations areas, leading to increased flow velocities and WSS values adjacents to plaques area.

4.2 Effect of Hemodynamic Parameters to Physiological Blood Flow

The hemodynamic parameters generate the formation of plaques that will break the circulation of blood and cause backflow in severe cases. The velocity of blood flow increased due to the formation of plaques that narrowing the lumen size. The lesion will induce atherosclerosis and within the time, the plaque becomes huge and forming a bulk of plaques, rupturing the coronary artery. Mohammad Nouri *et al.,* [8] were studying regarding atherosclerosis and sub-endothelial accumulation of low-density lipoprotein (LDL) molecules founded. There was disturbing blood flow where irregularities of WSS and velocities values happened. The authors used three pore models represented as endothelium boundary conditions, plasma flows and LDL transport. The endothelium pathways were divided into three divisions, known as leaky junctions, vesicles, and normal junctions. Based on their research, the LDL molecules that flow in endothelium layers passed through leaky junctions, forming LDL accumulation and increased atherosclerosis risk. They founded that the escaped LDL molecules mainly associated with the low WSS regions. Thus, resulting in interrupted flow conditions, where the percentages of total flow recorded were 5 %, 7 %, 14 %, 23 %, and 51 % respectively on the arterial branches where major disturbed flows happened. An experiment was conducted by Mohd Adib *et al.,* [7] showed a simulated physiological blood flow with different percentages of plaques blockage (20 %, 40 %, 60 %, and 90 %) was exactly imitated the real condition where the blood cannot reach full regions of coronary arteries. According to the authors, the patients may experiences shortness of breaths and other related CAD symptoms due to the formation of the

plaques. Based on Figure 1, the backflow of blood that happened due to the enormous regions conquered by plaques deposition with other invisible biomechanical forces changed simultaneously with the arising problems of atherosclerosis.

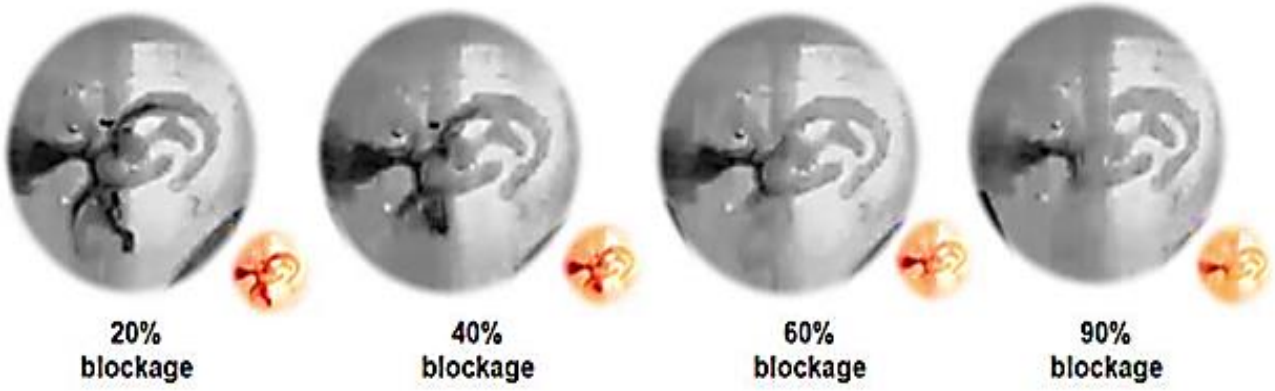

Fig. 1. Percentage of blocked coronary arteries due to the presence of plaques this image obtained from visual images using the *CardioVASS* device [7]

Figure 2 shows the effect of plaque formation in the coronary artery region. The atherosclerotic plaque caused differences in shear stress distribution. Incoming shear stress before plaque path is low and high when passing through atherosclerotic plaque from oscillatory shear stress after passing the plaque region. The oscillatory shear stress then resulting in the formation of a vortex in the coronary artery region. The irregularities form in the coronary artery were due to the plaque formation that may result in inflammation and other symptoms related to the patient-specific CAD.

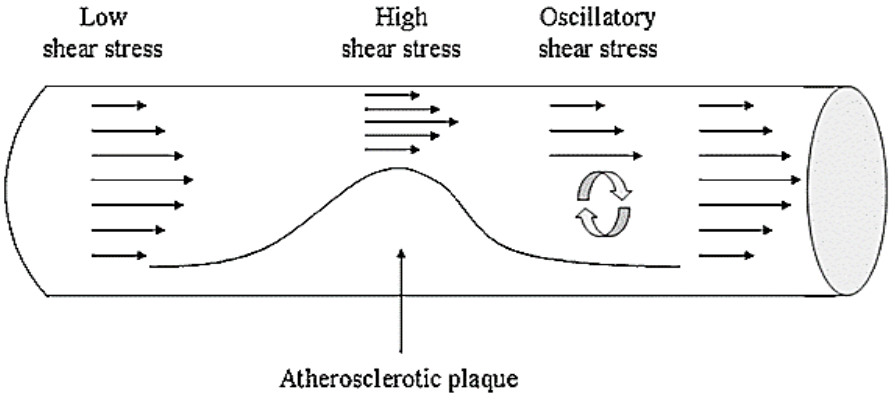

Fig. 2. Differential distribution of shear stress proximal to a lumen-protruding atherosclerotic plaque in a normal arterial segment [1]

Figure 3 shows the coronary artery model using CFD analysis where the formation of the possible plaques may occur as stated in (a) and (b). The diagram described the pre-plaque and post-plaque situations during the systolic and mid-diastolic peak of time (c) and (d). The red region in Figure 3 shows that the velocity was the highest in the region and the lowest velocity indicates the blue region. Plaque may happen in the region which had the highest velocity of blood flow and frequently appeared on the bifurcation of the coronary arteries where low WSS was developed [47].

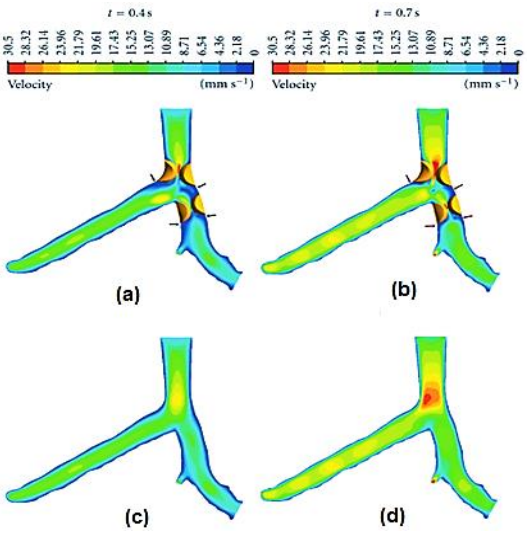

Fig. 3. Flow rate observed in simulated pre-plaque and post-plaque models at 0.4 s systolic maximum and 0.7 s mid-diastolic level (a)(b)(c)(d). Arrows indicate the anatomical locations where plaques can spread to low flow areas [12]

4.3 Limitations

The inconsistency of data gains influenced by many factors for instance variation of methods use, different assumptions of the physiological boundary of blood flow, agreement regarding mutual parameters for coronary artery and contradiction of geometry meshes in CFD. A big scale of studies must be conducted to ensure the reliability of the data used [48,49]. In the future, all of the limitations must be overcome to gain an accurate solution for CAD problems while the use of CFD analyses is not denied in contributing huge benefaction in solving CAD problems. The weaknesses identified from most of the previous research using the CFD analysis method were the setting of the parameters such as boundary conditions. Many researchers found that the prediction on the CFD parameter values was quite challenging [50]. Some researchers need to simulate a few more times to gain the exact parameters [51]. Major assumptions made by researchers are the inflow and outflow of the coronary artery model [52] that sometimes not identical to the patient's blood flow [53]. This will result in a different collection of data compared with real condition data. Another rising problem in the simulation process was choosing a precise method in developing accurate images of the CAD models.

5. Conclusions

In conclusion, the usage of CFD in determining CAD problems has brought a huge contribution especially in detected the main important hemodynamic parameters on physiological blood flow studies. Overall, the researchers achieved mutual agreements that WSS induces and activates the development of CAD accompanied by other hemodynamics parameters as mentioned earlier in Table 1 and Table 2. Low WSS acts as an initiator, before changing to median and high WSS that worsen the condition of the coronary artery by making the progression of plaque and increasing inflammatory symptoms for the patients. As WSS is a tangential factor, patients or researchers

cannot block the formation of atherosclerosis or CAD from happening but can study the symptoms and control lifestyles of patients.

Acknowledgment

The support of the Universiti Malaysia Pahang under grant RDU190805, KPT grant (PRGS/1/2019/KT03/UMP/02/4) and MedEHiT are gratefully acknowledged. By this opportunity, we would like to thank Mr. Idris Mat Sahat from Human Engineering Group, Universiti Malaysia Pahang for sharing valuable information following our research interest. We would face many difficulties without his assistance.

References

[1] Sun, Zhonghua, and Lei Xu. "Computational fluid dynamics in coronary artery disease." *Computerized medical imaging and graphics* 38, no. 8 (2014): 651-663. https://doi.org/10.1016/j.compmedimag.2014.09.002

[2] World Health Organization. "Cardiovascular diseases." origin.who.int

[3] Loh Foon Fong. "Heart attack leading cause of death." *The Star online*.

[4] Seong, Ang Choon, and Chan Kok Meng John. "A review of coronary artery disease research in Malaysia." *Med J Malaysia* 71, no. Supplement 1 (2016): 42-57.

[5] Papadopoulos, Konstantinos P., Manolis Gavaises, Ioannis Pantos, Demosthenes G. Katritsis, and Nicholas Mitroglou. "Derivation of flow related risk indices for stenosed left anterior descending coronary arteries with the use of computer simulations." *Medical engineering & physics* 38, no. 9 (2016): 929-939. https://doi.org/10.1016/j.medengphy.2016.05.016

[6] Samady, Habib, Parham Eshtehardi, Michael C. McDaniel, Jin Suo, Saurabh S. Dhawan, Charles Maynard, Lucas H. Timmins, Arshed A. Quyyumi, and Don P. Giddens. "Coronary artery wall shear stress is associated with progression and transformation of atherosclerotic plaque and arterial remodeling in patients with coronary artery disease." *Circulation* 124, no. 7 (2011): 779-788. https://doi.org/10.1161/CIRCULATIONAHA.111.021824

[7] Adib, Mohd Azrul Hisham Mohd, Khairul Shah Affendy Yakof, Zulfikar Anuar, Nizam Abdullah, Idris Mat Sahat, and Nur Hazreen Mohd Hasni. "The Cardio Vascular Simulator (CardioVASS) Device on Monitoring the Physiology of Blood Flow Circulation via Angiographic Image for Medical Trainee." *Journal of Advanced Research in Fluid Mechanics and Thermal Sciences 62,* no. 1 (2019): 103–111.

[8] Nouri, Mohammad, Farhang Jalali, Gholamreza Karimi, and Khalil Zarrabi. "Image-based computational simulation of sub-endothelial LDL accumulation in a human right coronary artery." *Computers in biology and medicine* 62 (2015): 206-221. https://doi.org/10.1016/j.compbiomed.2015.04.013

[9] Chaichana, Thanapong, Zhonghua Sun, and James Jewkes. "Computation of hemodynamics in the left coronary artery with variable angulations." *Journal of biomechanics* 44, no. 10 (2011): 1869-1878. https://doi.org/10.1016/j.jbiomech.2011.04.033

[10] Kim, Hyun J., I. E. Vignon-Clementel, C. A. Figueroa, K. E. Jansen, and C. A. Taylor. "Developing computational methods for three-dimensional finite element simulations of coronary blood flow." *Finite Elements in Analysis and Design* 46, no. 6 (2010): 514-525. https://doi.org/10.1016/j.finel.2010.01.007

[11] Tado, Radhe, Ashish B. Deoghare, and K. M. Pandey. "Computational Study of Blood Flow Analysis for Coronary Artery Disease." *International Journal of Biomedical and Biological Engineering* 12, no. 2 (2018): 35-39.

[12] Chaichana, Thanapong, Zhonghua Sun, and James Jewkes. "Computational fluid dynamics analysis of the effect of plaques in the left coronary artery." *Computational and mathematical methods in medicine* 2012 (2012): 1-9. https://doi.org/10.1155/2012/504367

[13] Schneiderbauer, Simon, and Michael Krieger. "What do the Navier–Stokes equations mean?." *European Journal of Physics* 35, no. 1 (2013): 015020. https://doi.org/10.1088/0143-0807/35/1/015020

[14] Doutel, E., S. I. S. Pinto, J. B. L. M. Campos, and J. M. Miranda. "Link between deviations from Murray's Law and occurrence of low wall shear stress regions in the left coronary artery." *Journal of theoretical biology* 402 (2016): 89-99. https://doi.org/10.1016/j.jtbi.2016.04.038

[15] Manoliu, Vasile. "Modeling cardiovascular hemodynamics in a model with nonlinear parameters." In *2015 E-Health and Bioengineering Conference (EHB)*, pp. 1-4. IEEE, 2015. https://doi.org/10.1109/EHB.2015.7391407

[16] Valdez-Jasso, Daniela, Daniel Bia, Yanina Zócalo, Ricardo L. Armentano, Mansoor A. Haider, and Mette S. Olufsen. "Linear and nonlinear viscoelastic modeling of aorta and carotid pressure–area dynamics under In vivo and ex vivo conditions." *Annals of biomedical engineering* 39, no. 5 (2011): 1438-1456. https://doi.org/10.1007/s10439-010-0236-7

[17] Gijsen, Frank JH, Jolanda J. Wentzel, Attila Thury, Bram Lamers, Johan CH Schuurbiers, Patrick W. Serruys, and Antonius F. Van der Steen. "A new imaging technique to study 3-D plaque and shear stress distribution in human coronary artery bifurcations in vivo." *Journal of biomechanics* 40, no. 11 (2007): 2349-2357. https://doi.org/10.1016/j.jbiomech.2006.12.007

[18] Liu, Guiying, Jianhuang Wu, Dhanjoo N. Ghista, Wenhua Huang, and Kelvin KL Wong. "Hemodynamic characterization of transient blood flow in right coronary arteries with varying curvature and side-branch bifurcation angles." *Computers in biology and medicine* 64 (2015): 117-126. https://doi.org/10.1016/j.compbiomed.2015.06.009

[19] Kumar, Arnav, Olivia Y. Hung, Marina Piccinelli, Parham Eshtehardi, Michel T. Corban, David Sternheim, Boyi Yang et al. "Low coronary wall shear stress is associated with severe endothelial dysfunction in patients with nonobstructive coronary artery disease." *JACC: Cardiovascular Interventions* 11, no. 20 (2018): 2072-2080. https://doi.org/10.1016/j.jcin.2018.07.004

[20] Kumar, Arnav, Elizabeth W. Thompson, Adrien Lefieux, David S. Molony, Emily L. Davis, Nikita Chand, Stephane Fournier et al. "High coronary shear stress in patients with coronary artery disease predicts myocardial infarction." *Journal of the American College of Cardiology* 72, no. 16 (2018): 1926-1935. https://doi.org/10.1016/j.jacc.2018.07.075

[21] Wellnhofer, E., L. Goubergrits, U. Kertzscher, K. Affeld, and E. Fleck. "Novel non-dimensional approach to comparison of wall shear stress distributions in coronary arteries of different groups of patients." *Atherosclerosis* 202, no. 2 (2009): 483-490. https://doi.org/10.1016/j.atherosclerosis.2008.05.044

[22] Martin, D., A. Zaman, J. Hacker, D. Mendelow, and D. Birchall. "Analysis of haemodynamic factors involved in carotid atherosclerosis using computational fluid dynamics." *The British Journal of Radiology* 82, no. special_issue_1 (2009): S33-S38. https://doi.org/10.1259/bjr/59367266

[23] Chiu, Jeng-Jiann, and Shu Chien. "Effects of disturbed flow on vascular endothelium: pathophysiological basis and clinical perspectives." *Physiological reviews* 91, no. 1 (2011): 327-387. https://doi.org/10.1152/physrev.00047.2009

[24] Steinman, David A., and Charles A. Taylor. "Flow imaging and computing: large artery hemodynamics." *Annals of biomedical engineering* 33, no. 12 (2005): 1704-1709. https://doi.org/10.1007/s10439-005-8772-2

[25] Boyd, Joshua, James M. Buick, and Simon Green. "Analysis of the Casson and Carreau-Yasuda non-Newtonian blood models in steady and oscillatory flows using the lattice Boltzmann method." *Physics of Fluids* 19, no. 9 (2007): 093103. https://doi.org/10.1063/1.2772250

[26] O. Kedem and A. Katchalsky. "Thermodynamic analysis of the permeability of biological membranes to non-electrolytes." *Biochimica et Biophysica Acta 27*, (1958): 229-246. https://doi.org/10.1016/0006-3002(58)90330-5

[27] Rybicki, Frank J., Simone Melchionna, Dimitris Mitsouras, Ahmet U. Coskun, Amanda G. Whitmore, Michael Steigner, Leelakrishna Nallamshetty et al. "Prediction of coronary artery plaque progression and potential rupture from 320-detector row prospectively ECG-gated single heart beat CT angiography: Lattice Boltzmann evaluation of endothelial shear stress." *The International Journal of Cardiovascular Imaging* 25, no. 2 (2009): 289-299. https://doi.org/10.1007/s10554-008-9418-x

[28] Asakura, Toshihisa, and Takeshi Karino. "Flow patterns and spatial distribution of atherosclerotic lesions in human coronary arteries." *Circulation research* 66, no. 4 (1990): 1045-1066. https://doi.org/10.1161/01.RES.66.4.1045

[29] Cancel, Limary M., Andrew Fitting, and John M. Tarbell. "In vitro study of LDL transport under pressurized (convective) conditions." *American Journal of Physiology-Heart and Circulatory Physiology* 293, no. 1 (2007): H126-H132. https://doi.org/10.1152/ajpheart.01188.2006

[30] Cecchi, Emanuele, Cristina Giglioli, Serafina Valente, Chiara Lazzeri, Gian Franco Gensini, Rosanna Abbate, and Lucia

Mannini. "Role of hemodynamic shear stress in cardiovascular disease." *Atherosclerosis* 214, no. 2 (2011): 249-256. https://doi.org/10.1016/j.atherosclerosis.2010.09.008

[31] Chatzizisis, Yiannis S., Ahmet Umit Coskun, Michael Jonas, Elazer R. Edelman, Charles L. Feldman, and Peter H. Stone. "Role of endothelial shear stress in the natural history of coronary atherosclerosis and vascular remodeling: molecular, cellular, and vascular behavior." *Journal of the American College of Cardiology* 49, no. 25 (2007): 2379-2393.
https://doi.org/10.1016/j.jacc.2007.02.059

[32] Chien, Shu. "Molecular and mechanical bases of focal lipid accumulation in arterial wall." *Progress in biophysics and molecular biology* 83, no. 2 (2003): 131-151.
https://doi.org/10.1016/S0079-6107(03)00053-1

[33] Gimbrone Jr, Michael A., James N. Topper, Tobi Nagel, Keith R. Anderson, and Guillermo Garcia-Cardeña. "Endothelial dysfunction, hemodynamic forces, and atherogenesis a." *Annals of the new york academy of sciences* 902, no. 1 (2000): 230-240.
https://doi.org/10.1111/j.1749-6632.2000.tb06318.x

[34] Kaazempur-Mofrad, M. R., and C. R. Ethier. "Mass transport in an anatomically realistic human right coronary artery." *Annals of Biomedical Engineering* 29, no. 2 (2001): 121-127.
https://doi.org/10.1114/1.1349704

[35] Knight, Joseph, Ufuk Olgac, Stefan C. Saur, Dimos Poulikakos, William Marshall Jr, Philippe C. Cattin, Hatem Alkadhi, and Vartan Kurtcuoglu. "Choosing the optimal wall shear parameter for the prediction of plaque location—a patient-specific computational study in human right coronary arteries." *Atherosclerosis* 211, no. 2 (2010): 445-450. https://doi.org/10.1016/j.atherosclerosis.2010.03.001

[36] Papafaklis, Michail I., Konstantinos C. Koskinas, Yiannis S. Chatzizisis, Peter H. Stone, and Charles L. Feldman. "In-vivo assessment of the natural history of coronary atherosclerosis: vascular remodeling and endothelial shear stress determine the complexity of atherosclerotic disease progression." *Current opinion in cardiology* 25, no. 6 (2010): 627-638.
https://doi.org/10.1097/HCO.0b013e32833f0236

[37] Levesque, M. J. "Liepsch D, Moravec S, Nerem RM." *Correlation of endothelial cell shape and wall shear stress in a stenosed dog aorta. Arteriosclerosis* 6 (1986): 220-229.
https://doi.org/10.1161/01.ATV.6.2.220

[38] Corno, Antonio F., Christian Vergara, Chellappan Subramanian, Robert A. Johnson, Tiziano Passerini, Alessandro Veneziani, Luca Formaggia, Nelson Alphonso, Alfio Quarteroni, and Jonathan C. Jarvis. "Assisted Fontan procedure: animal and in vitro models and computational fluid dynamics study." *Interactive cardiovascular and thoracic surgery* 10, no. 5 (2010): 679-684.
https://doi.org/10.1510/icvts.2009.223024

[39] Murray, Cecil D. "The physiological principle of minimum work applied to the angle of branching of arteries." *The Journal of general physiology* 9, no. 6 (1926): 835-841.
https://doi.org/10.1085/jgp.9.6.835

[40] Murray, Cecil D. "The physiological principle of minimum work: I. The vascular system and the cost of blood volume." *Proceedings of the National Academy of Sciences of the United States of America* 12, no. 3 (1926): 207-214.
https://doi.org/10.1073/pnas.12.3.207

[41] Britannica. "Magnetohydrodynamics" Britannica.com

[42] Adib, M. A. H. M., and Nur Hazreen Mohd Hasni. "Modeling of Blood Flow Velocity into the Main Artery via Left Ventricle of Heart during Steady Condition." *World Academy of Science, Engineering and Technology, International Journal of Medical, Health, Biomedical, Bioengineering and Pharmaceutical Engineering* 6, no. 4 (2012): 97-101.

[43] Belloni, Francis L. "Teaching the principles of hemodynamics." *Advances in Physiology education* 277, no. 6 (1999): S187.
https://doi.org/10.1152/advances.1999.277.6.S187

[44] Adib, Mohd Azrul Hisham Mohd, Kahar Osman, and Rudiyanto Philman Jong. "Analysis of blood flow into the main artery via mitral valve: Fluid structure interaction model." In *2010 International Conference on Science and Social Research (CSSR 2010)*, pp. 356-360. IEEE, 2010.

[45] VanderLaan, Paul A., Catherine A. Reardon, and Godfrey S. Getz. "Site specificity of atherosclerosis: site-selective responses to atherosclerotic modulators." *Arteriosclerosis, thrombosis, and vascular biology* 24, no. 1 (2004): 12-22.
https://doi.org/10.1161/01.ATV.0000105054.43931.f0

[46] Ohayon, Jacques, Ahmed M. Gharib, Alberto Garcia, Julie Heroux, Saami K. Yazdani, Mauro Malvè, Philippe Tracqui et al. "Is arterial wall-strain stiffening an additional process responsible for atherosclerosis in coronary

bifurcations?: an in vivo study based on dynamic CT and MRI." *American Journal of Physiology-Heart and Circulatory Physiology* 301, no. 3 (2011): H1097-H1106.
https://doi.org/10.1152/ajpheart.01120.2010

[47] Steinman, David A. "Image-based computational fluid dynamics modeling in realistic arterial geometries." *Annals of biomedical engineering* 30, no. 4 (2002): 483-497.
https://doi.org/10.1114/1.1467679

[48] Adib, M. A. H. M., Kahar Osman, Nur Hazreen Mohd Hasni, Oteh Maskon, Faradila Naim, Zulkifli Ahmad, Idris Sahat, and A. N. Mu'tasim. "Computational Simulation of Heart Valve Leaflet under Systole Condition using Fluid Structure Interaction Model." In *International Conference on Computer Engineering and Bioinformatics*. 2011.

[49] Adib, Mohd, Mohd Azrul Hisham, Mohd Hasni, and Nur Hazreen. "Degenerative vs rigidity on mitral valve leaflet using fluid structure interaction (FSI) model." In *Journal of Biomimetics, Biomaterials and Biomedical Engineering*, vol. 26, pp. 60-65. Trans Tech Publications Ltd, 2016.
https://doi.org/10.4028/www.scientific.net/JBBBE.26.60

[50] Mahrous, Samar A., Nor Azwadi Che Sidik, and M. Saqr Khalid. "Newtonian and non-Newtonian CFD Models of Intracranial Aneurysm: A Review." *CFD Letters* 12, no. 1 (2020): 62-86.

[51] Paramasivam, Vijayajothi, Nenad Filipovic, Kanesan Muthusamy, and Mohammed Rafiq Abdul Kadir54. "Finite Element Computation for Solving Pulsatile Blood Flow: Relevance in Assessing the Flow Dynamics in Abdominal Aortic Aneurysms." *CFD Letters* 2, no. 4 (2010): 149-162.

[52] Hansson, Göran K. "Inflammation, atherosclerosis, and coronary artery disease." *New England Journal of Medicine* 352, no. 16 (2005): 1685-1695.
https://doi.org/10.1056/NEJMra043430

[53] Hong, Lim Sheh, Mohd Azrul Hisham Mohd Adib, Mohd Shafie Abdullah, and Radhiana Hassan. "Qualitative and Quantitative Comparison of Hemodynamics Between MRI Measurement and CFD Simulation on Patient-specific Cerebral Aneurysm–A Review." *Journal of Advanced Research in Fluid Mechanics and Thermal Sciences 68*, no. 2 (2020): 112-123.
https://doi.org/10.37934/arfmts.68.2.112123